

# AC and DC Conductivity Anisotropies in Lightly Doped $\text{La}_{2-x}\text{Sr}_x\text{CuO}_4$

M. B. Silva Neto,<sup>1,\*</sup> G. Blumberg,<sup>2</sup> A. Gozar,<sup>3</sup> Seiki Komiya,<sup>4</sup> and Yoichi Ando<sup>5</sup>

<sup>1</sup>*Institut für Theoretische Physik, Universität Stuttgart, Pfaffenwaldring 57, 70550, Stuttgart, Germany*

<sup>2</sup>*National Institute of Chemical Physics and Biophysics, Akadeemia tee 23, 12618 Tallinn, Estonia*

<sup>3</sup>*Brookhaven National Laboratory, Upton, New York 11973-5000, USA*

<sup>4</sup>*Central Research Institute of Electric Power Industry, Yokosuka, Kanagawa 240-0196, Japan*

<sup>5</sup>*Institute of Scientific and Industrial Research, Osaka University, Ibaraki, Osaka 567-0047, Japan*

The AC and DC conductivity anisotropies in the low temperature orthorhombic phase of lightly doped  $\text{La}_{2-x}\text{Sr}_x\text{CuO}_4$  are ascribed to the rotational symmetry broken, localized impurity states resulting from the trapping of doped holes by Sr ions. The two lowest-energy  $p$ -wave-like states are split by orthorhombicity and partially filled with holes. This leaves a unique imprint in AC conductivity, which shows two distinct infrared continuum absorption energies. Furthermore, the existence of two independent channels for hopping conductivity, associated to the two orthorhombic directions, explains quantitatively the observed low temperature anisotropies in DC conductivity.

PACS numbers: 78.30.-j, 74.72.Dn, 63.20.Ry, 63.20.dk

*Introduction* – Understanding the evolution from a Mott insulating behavior until the realization of high temperature superconductivity in lamellar copper-oxides is one of the most challenging problems in condensed matter physics. It is widely agreed that  $t - J$ -like models already capture the essential features of underdoped cuprates [1], such as a Fermi surface (FS) composed of small pockets [2]. However, while the rather low frequency of quantum Hall oscillations observed in  $\text{YBa}_2\text{Cu}_3\text{O}_{6.5}$  [3], as well as de Haas-van Alphen effect [4], support the small FS scenario, the validity of such strong coupling, single band description has been recently put under scrutiny, after a new analysis of the optical conductivity spectra in  $\text{La}_{2-x}\text{Sr}_x\text{CuO}_4$  [5]. Further information can also be obtained through a careful analysis of magnetic, optical, and transport experiments, such as the ones performed in untwinned  $\text{La}_{2-x}\text{Sr}_x\text{CuO}_4$  single crystals, the simplest representative of this class of compounds [6]. Understanding these experiments might ultimately help us clarify the role of interactions in cuprates.

Infrared (IR) spectroscopy is a very useful tool to investigate the charge dynamics in metals and semiconductors. The analysis of the AC conductivity spectrum of  $\text{La}_{2-x}\text{Sr}_x\text{CuO}_4$ , for  $x = 0.03$  and  $0.04$ , by Dumm *et al.* [7], revealed that: i) at high temperature,  $T > 80$  K, a Drude-like response is observed, suggesting that the electronic conductivity is bandlike even for such low doping, which is consistent with the mobility analysis of the DC conductivity [8]; ii) at lower temperature, instead, the suppression of the Drude-like behavior in the far IR, with the observation of a peak centered at finite frequency  $\omega$ , points towards the localization of the charge carriers [9], much like as it happens in doped semiconductors. The position of such peak can be associated to the typical energy scale for localization, the binding energy of the holes. Most remarkable, however, is the observation of *two distinct absorption energies* for light polarized along the two orthorhombic axis,  $A-$  and  $B-$  channels [7].

The DC conductivity in lightly doped  $\text{La}_{2-x}\text{Sr}_x\text{CuO}_4$  can also be divided into two main regimes: metallic (bandlike) and insulating (hopping) [8, 10]. At higher to moderate temperatures, a simple Drude picture for the hole conductivity,  $\sigma = ne^2\tau/m^*$ , is able to explain (surprisingly) quite well the rather weakly anisotropic DC conductivity data. At lower temperature, however, when the holes localize, hopping conductivity between impurity sites becomes the main mechanism for the transport, which is found to be clearly anisotropic and also exhibits *two different temperature scales* for the onset of localization [10], also called *freezing-out temperatures* [12], depending on the direction of the applied electric field.

In this letter we unveil the mechanism behind the unusual and anisotropic charge dynamics in lightly doped  $\text{La}_{2-x}\text{Sr}_x\text{CuO}_4$ , summarized in the two preceding paragraphs. We demonstrate that the two energy scales found in the AC response are associated to the two lowest-energy, parity-odd, rotational-symmetry-broken  $p$ -wave impurity states for holes trapped by Sr ions in  $\text{La}_{2-x}\text{Sr}_x\text{CuO}_4$ . Furthermore, we show that the existence of two independent impurity channels for hopping conductivity, explains naturally the low temperature DC conductivity anisotropies [10]. The relationship between a rotational non-invariant impurity state and anisotropic DC response was first acknowledged by Kotov and Sushkov, who considered the deformation of a single, parity-even, Hydrogenic  $1s$  orbital due to spiral correlations [11]. As we shall soon see, the selection rules for IR absorption, and the optical spectrum, are consistent, instead, with two parity-odd  $p$ -wave functions [7].

*Electronic Structure* – According to exact diagonalization studies for the  $t - t' - J$  model on a square lattice [13, 14, 15], the ground state for a hole bound to a Sr charged impurity at the center of a 4-Cu plaquette is doubly-degenerate and parity-odd. The presence of the Sr impurity breaks the translational symmetry of the square lattice and the different possible localized states

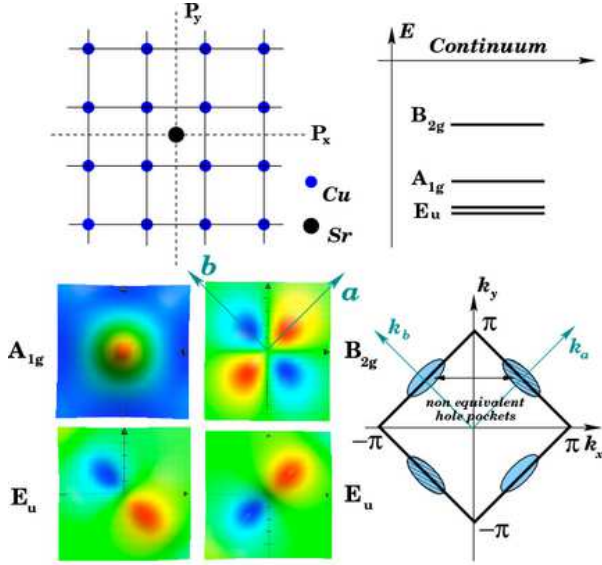


FIG. 1: (Color online) Top-Left: Sr ion at the center of a 4-Cu plaquette and the reflection axis  $P_x$ ,  $P_y$ . Top-Right: Localized energy levels and their irreducible representations of the  $D_{4h}$  point group. The ground state  $E_u$  is doubly degenerate and parity odd (note that we are using the hole picture here, so the energy axis is reversed). Bottom-Left:  $A_{1g}$ ,  $B_{2g}$ , and  $E_u$  wave functions. Bottom-Right: The delocalized hole has dispersion with maxima at  $(\pm\pi/2, \pm\pi/2)$  and belongs to  $B_{2g}$ .

can be classified according to the irreducible representations of the  $C_{4v}$  point group, labeled by the eigenvalues of the reflection operators  $P_x$  and  $P_y$ ,  $(P_x, P_y)$  [15]. The doubly-degenerate ground state belongs then to the two-dimensional  $E$  representation and corresponds to the degenerate  $(+, -)$  and  $(-, +)$  states [13, 15]. There is a low-lying excited  $s$ -wave state which belongs to  $A_1$ , labeled by  $(+, +)$ , and a higher energy  $d$ -wave state belonging to  $B_2$ , labeled by  $(-, -)$  [15]. For the continuum part, the single delocalized hole state of the  $t - t' - J$  model is labelled by its momentum  $\mathbf{k}$  and corresponds to the maxima of the parity-even elliptical hole pockets centered at  $(\pm\pi/2, \pm\pi/2)_g$  (in units  $a = 1$ ), see Fig. 1.

In what follows, however, it will be more convenient to consider explicitly the symmetry reduction in  $\text{La}_{2-x}\text{Sr}_x\text{CuO}_4$  from the high temperature tetragonal (HTT) phase, with crystal structure  $I4/mmm$  and point group  $D_{4h}$ , down to the low temperature orthorhombic (LTO) phase, with  $Bmab$  crystal structure ( $a$  and  $b$  are the two planar orthorhombic axis shown in Fig. 1, with  $b > a$ ) and associated  $D_{2h}$  point group. In this case, the double degeneracy of the ground state is lifted by the orthorhombicity, and the character of the parity-odd ground state is reduced following  $E_u \rightarrow B_{2u} + B_{3u}$ . Analogously, the higher energy states are reduced according to  $A_{1g} \rightarrow A_g^s$  and  $B_{2g} \rightarrow A_g^d$ . Finally, also the single delocalized hole state, labelled by  $(\pm\pi/2, \pm\pi/2)_g$ , has its symmetry modified from  $B_{2g} \rightarrow A_g$ .

Following Kohn and Luttinger (KL) [16], the wave functions corresponding to the  $i = B_{3u}, B_{2u}, A_g^s, A_g^d$  states can be generally written as  $\Psi_i = \sum_{\mu} \alpha_{\mu}^i F_{\mu}^i(\mathbf{r}) \phi(\mathbf{k}_{\mu}, \mathbf{r})$ , where  $\phi(\mathbf{k}_{\mu}, \mathbf{r}) = e^{i\mathbf{k}_{\mu} \cdot \mathbf{r}} u_{\mathbf{k}_{\mu}}(\mathbf{r})$  and  $u_{\mathbf{k}_{\mu}}(\mathbf{r})$  is a periodic Bloch wave function with minima at  $\mathbf{k}_{\mu} = \mathbf{k}_{a,b}^{\pm}$ . The index  $\mu$  runs over the  $\mathbf{k}_a^+ = (\pi/2, \pi/2)$ ,  $\mathbf{k}_b^+ = (-\pi/2, \pi/2)$ ,  $\mathbf{k}_a^- = (-\pi/2, -\pi/2)$ , and  $\mathbf{k}_b^- = (\pi/2, -\pi/2)$  pockets, and the envelope functions read  $F_{\mu}^i(\mathbf{r}) = (\pi\xi^2)^{-1/2} e^{-r/\xi^i}$ , where  $\xi^i$  controls the exponential decay of the wave function for the  $i$ -th impurity level. The parity-odd coefficients,  $\alpha_{\mu}^{B_{3u}} = (1/2)(1, 0, -1, 0)$  and  $\alpha_{\mu}^{B_{2u}} = (1/2)(0, 1, 0, -1)$ , as well as the parity-even ones,  $\alpha_{\mu}^{A_g^s} = (1/4)(1, 1, 1, 1)$  and  $\alpha_{\mu}^{A_g^d} = (1/4)(1, -1, 1, -1)$ , are determined by the relevant symmetries of the  $Bmab$  point group [16]. The KL  $\Psi_i$  wave functions (see Fig. 1) do not include, however, the information that the holes are incoherent over a large part of the pockets [2]. These effects will be reported elsewhere and for now it suffices to acknowledge the  $p$ -orbital shape of the lowest energy impurity states.

The orthorhombic splitting  $E_u \rightarrow B_{3u} + B_{2u}$  is determined by the competition between the Coulomb potential from the Sr ion, which favors a  $B_{3u}$  ground state ( $b > a$ ), and the next-to-nearest-neighbor hopping  $t'_a > t'_b$  [17], which favors a  $B_{2u}$  ground state. In what follows we shall argue that: i) for  $x = 0.01$ , when the Sr ion is poorly screened, the  $B_{3u}$  state becomes the ground state; ii) for  $x = 0.03$ , instead, the  $B_{2u}$  state becomes the ground state (most likely due to better screening), causing a switch of the DC conductivity anisotropies (a related switch is also observed in the Raman intensity anisotropies [19]).

**AC spectrum and IR Selection Rules** – The finite frequency peaks observed in the AC spectrum of  $\text{La}_{2-x}\text{Sr}_x\text{CuO}_4$  for  $x = 0.03, 0.04$  [7] are related to the absorption, by the continuum, of the photoionized hole states, made possible by the electric-dipole coupling. Within the framework of the  $D_{2h}$  group, a dipole along the  $a/b$  axis belongs to the  $B_{3u}/B_{2u}$  irreducible representations, respectively. Since the single delocalized hole belongs to  $A_g$ , the only allowed electric dipole transitions are: i) absorption of a  $B_{3u}$  hole for  $E \parallel a$ , since  $B_{3u} \times B_{3u} = A_g$ ; ii) absorption of a  $B_{2u}$  hole for  $E \parallel b$ , also because  $B_{2u} \times B_{2u} = A_g$ , see Fig. 2, determining unambiguously the odd parity of the ground state.

The energy difference between the AC peaks at  $\varepsilon_0 - \varepsilon_A$ , for the  $A$ - channel, and at  $\varepsilon_0 - \varepsilon_B$ , for the  $B$ - channel, is a direct measure of the orthorhombic level splitting. For  $x = 0.03, 0.04$  such splitting is  $\sim 30$  K [7], and the  $B_{3u}$  state is shallower than the  $B_{2u}$  state, see Fig. 2. For  $x = 0.01$ , in turn, we shall argue that this situation is reversed, causing the DC anisotropy switch [19].

**Disorder Bandwidth** – Each Sr ion doped into  $\text{La}_{2-x}\text{Sr}_x\text{CuO}_4$  acts as an acceptor and introduces precisely one hole into the system. Nevertheless, a sizable bandwidth of disorder  $W$  can allow for unoccupied accep-

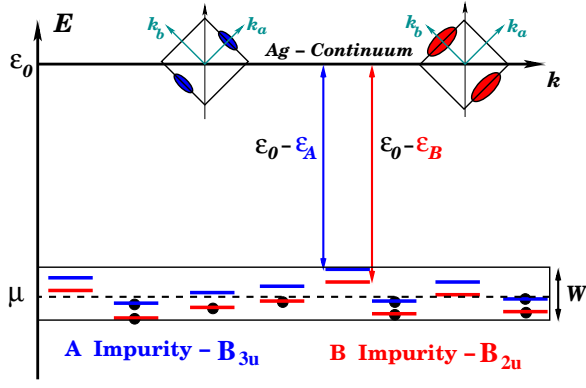


FIG. 2: (Color online) Localized deep and shallow acceptor states, as well as continuum states, for  $x = 0.03$  (again, the energy axis is reversed). A bandwidth  $W$  allows for empty sites above  $\mu$  and sites with two holes below  $\mu$ . Both  $B_{2u}$  and  $B_{3u}$  states are partially occupied at  $T = 0$ , in fractions  $\delta_A$  and  $\delta_B$ , and provide different populations of pockets at  $T \neq 0$ .

tor sites above the chemical potential and, as imposed by charge neutrality, acceptor sites with two holes below it, see Fig. 2. Observe that even though double occupancy of the  $B_{2u}$  or  $B_{3u}$  levels is forbidden due to the large on-site Coulomb repulsion  $U$ , the rather large size of the two *orthogonal*  $p$ -wave-like orbitals allows for the presence of one hole at each of the  $B_{2u}$  and  $B_{3u}$  levels, independently, with small energy cost. More importantly, the fraction (or percentage) of empty  $B_{2u}$  states above  $\mu$  in Fig. 2,  $1 - \delta_B$ , is the same as of filled  $B_{3u}$  states below it,  $\delta_A$ , such that *the number of carriers participating in hopping conductivity for both channels is the same*.

**Hopping Regime** – The conductance due to phonon assisted hopping between two  $p$ -wave like orbitals at sites  $i$  and  $j$ , separated by a distance  $\mathbf{R}_{ij}$ , reads

$$G_{ij} = G_0^\sigma \cos^4 \Theta_{ij} \left\{ e^{-\Delta E_{ij}/k_B T} e^{-2R_{ij}/\xi} \right\}, \quad (1)$$

where  $\Delta E_{ij}$  is the energy difference between the two impurity sites, and  $\Theta_{ij}$  is the angle between  $\mathbf{R}_{ij}$  and the directions of the  $p$ -orbitals. Here we considered only  $\sigma$ -type overlaps,  $G_0^\sigma$ , and neglected the weaker  $\pi$ -type overlaps.

When the temperature is still reasonably high the hole at site  $i$  can hop to its nearest impurity site  $j$ , as long as this is not already occupied, in the *nearest impurity hopping* (NIH) regime [20]. The conductivity is calculated by replacing in (1):  $\langle R_{ij} \rangle = \tilde{R}$ ,  $\langle \Delta E_{ij} \rangle = \epsilon_c$ , and averaging out  $\langle \cos^4 \Theta_{ij} \rangle$ , where  $\tilde{R}$  and  $\epsilon_c$  are, respectively, the average inter-impurity distance and energy difference

$$\sigma_{NIH}(T) = \sigma_0 \exp \left[ - \left( \frac{\epsilon_c}{k_B T} \right) \right]. \quad (2)$$

When the temperature is very small, however,  $G_{ij}$  is determined by the critical conductance  $G_c$  of a percolated random resistance network (RRN) [21]. In this case,

the maximum: i) carrier jump distance  $R_{max}$ , ii) energy difference  $\Delta E_{max}$ , and iii) angle  $\Theta_{max}$ , are constrained through the density of states. The result is Mott's *variable range hopping* (VRH), that for  $d = 2$  reads [12]

$$\sigma_{VRH}(T) = \sigma_0 \exp \left[ - \left( \frac{T_0}{T} \right)^{1/3} \right], \quad (3)$$

where  $T_0 = 13.8/k_B N_\Theta(\mu) \xi^2$ , and  $N_\Theta(\mu)$  is the constant density of states close to the Fermi level within the solid angle determined by  $2\Theta_{max}$  (for the isotropic VRH case  $2\Theta_{max} = 2\pi$ ). Both  $\epsilon_c$  and  $T_0$  decrease with doping, and the crossover between NIH and VRH regimes occurs at  $\epsilon_c = -d \ln(\sigma_{VRH}(T))/d\beta$ , with  $\beta = 1/k_B T$  [20].

**DC Hopping Conductivity Anisotropy** – The DC conductivity for arbitrary direction of the electric field receives contribution from both channels,  $\sigma_{B_{2u}}(T)$  and  $\sigma_{B_{3u}}(T)$ , where  $\sigma_{(B_{2u}, B_{3u})}(T)$  are hopping conductivities between two  $B_{(2u, 3u)} \rightarrow B_{(2u, 3u)}$  states, either NIH or VRH, which is assisted by the strong  $A_g$  phonons, while the cross hopping between  $B_{2u} \rightleftharpoons B_{3u}$  will be neglected, since these involve the much weaker  $B_{1g}$  phonons.

Most importantly, since the conductivity is proportional to the square of the carrier distance jump projection into the direction of the electric field,  $(\mathbf{R}_{ij} \cdot \hat{\mathbf{e}})^2$ ,

$$\sigma_{B_{2u}}^{\hat{\mathbf{e}}} = \sigma_{B_{2u}}^{VRH}(T) \int_{-\Theta_{max}}^{\Theta_{max}} \cos^4 \Theta \cos^2(\beta - \Theta) d\Theta, \quad (4)$$

where  $\beta$  is the angle between  $\hat{\mathbf{e}}$  and the  $B_{2u}$  orbital (for the  $B_{3u}$  case we would have  $\sin^2(\beta - \Theta)$  instead). Now, for  $E \parallel a, b$  and  $\Theta_{max} \ll \pi/4$ , we have  $\sigma_{B_{3u}}^a / \sigma_{B_{3u}}^b \gg 1$ , for the  $B_{3u}$  channel, and  $\sigma_{B_{2u}}^a / \sigma_{B_{2u}}^b \ll 1$ , for the  $B_{2u}$  channel, showing that the conductivity for  $E \parallel a$  is dominated by  $\sigma_A(T) \approx \sigma_{B_{3u}}^a(T)$ , while for  $E \parallel b$  it is dominated by  $\sigma_B(T) \approx \sigma_{B_{2u}}^b(T)$ . Finally, the orthorhombic splitting between these two channels, with  $\xi_{B_{3u}} \neq \xi_{B_{2u}}$ , renders the DC hopping conductivity anisotropic.

**Drude Regime** – At high temperature the doped holes are ionized from the  $B_{3u}$  and  $B_{2u}$  impurity levels, to occupy the valence band pocket states at  $\mathbf{k}_a^\pm$  and  $\mathbf{k}_b^\pm$ , respectively, see Fig. 2. For  $E \parallel a(b)$ , the transport is dominantly due to the coherent holes with momenta along  $\mathbf{k}_a(\mathbf{k}_b)$  and mass  $m^*$ , and a simple Drude model

$$\sigma_{Drude}^{A,B} = \frac{\langle n_{2D}^{A,B} \rangle e^2 \tau}{c_0 m^*}, \quad (5)$$

suffices to describe the experimental data. Here  $e$  is the electric charge,  $c_0 = 6.6 \text{ \AA}$  is the interlayer distance, and  $1/\tau$  is the relaxation rate. The thermal activation of carriers is considered through the average thermal occupation  $\langle n_{2D}^{A,B} \rangle = 2n_{2D}^0 \delta_{A,B} / (1 + \sqrt{1 + 4g(n_{2D}^0/\mathcal{N}_0) e^{\beta \epsilon_f^{A,B}}})$ , where  $g = 2$  accounts for pseudospin (sublattice) degeneracy,  $\mathcal{N}_0 = N_0 T$ , with  $N_0$  being the two dimensional density of states,  $\delta_{A,B}$  are the  $T = 0$  fractions of  $B_{3u, 2u}$

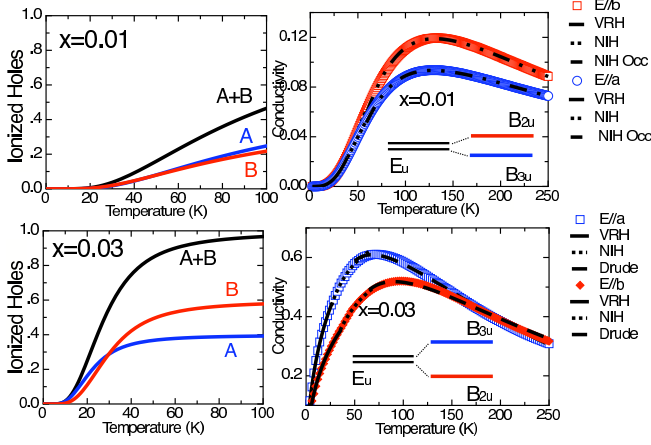


FIG. 3: (Color online) Fraction of thermally ionized holes and DC conductivities in  $(\text{m}\cdot\Omega\cdot\text{cm})^{-1}$ , for  $x = 0.01, 0.03$ .

impurities, satisfying  $\delta_A + \delta_B = 1$ ,  $\varepsilon_f^{A,B} = (\varepsilon_0 - \varepsilon_{A,B})$  are the *freezing out* (or binding) energies, and  $n_{2D}^0 = x/a^2$ .

*Comparison with Experiments* – In Fig. 3 we show the comparison between theory and DC conductivity data for  $x = 0.01, 0.03$ . For  $4g(n_{2D}^0/N_0)e^{\beta\varepsilon_f^{A,B}} \gg 1$ , low  $T$ ,  $\sigma_{Drude}$  is exponentially suppressed and the data are well fitted using the  $\sigma_{VRH}$  and  $\sigma_{NIH}$  expressions (3) and (2), respectively. For  $4g(n_{2D}^0/N_0)e^{\beta\varepsilon_f^{A,B}} \ll 1$ , instead, at higher  $T$ , when almost the totality of holes are ionized,  $\sigma_{Drude}$  dominates and we can use Eq. (5). Finally, we use  $1/\tau(T)$  data obtained from fits to the mobility  $\mu = e\tau/m^*$  [8], which can be well parametrized by the simple Fermi liquid expression  $1/\tau(T) = 1/\tau_0 + \alpha T^2$ .

For  $x = 0.01$  we find: i)  $T_0^A = 32829$  K,  $\varepsilon_c^A = 125.09$  K, and  $\delta_A = 0.52$ , for  $E \parallel a$ , and ii)  $T_0^B = 30878$  K,  $\varepsilon_c^B = 99.97$  K, and  $\delta_B = 0.48$ , for  $E \parallel b$ . Notice that the ratio  $T_0^A/T_0^B = \varepsilon_f^A/\varepsilon_f^B > 1$ , indicating that the  $B_{3u}$  state is the ground state, is slightly more populated, and the  $B_{3u}$  and  $B_{2u}$  splitting is very small. Here we used  $\varepsilon_f^A = 200$  K and  $\varepsilon_f^B \approx 180$  K, and  $N_0 \approx 1.8 \times 10^{-3} \text{K}^{-1}/a^2$ . We note that the NIH regime extends up to 250 K, when weighed by the thermal occupation of local levels.

For  $x = 0.03$  we find: i)  $T_0^A = 94.38$  K,  $\varepsilon_c^A = 15.2$  K, and  $\delta_A = 0.4$ , for  $E \parallel a$ , and ii)  $T_0^B = 107.2$  K,  $\varepsilon_c^B = 24.1$  K, and  $\delta_B = 0.6$ , for  $E \parallel b$ . Notice that we now have  $T_0^A/T_0^B = \varepsilon_f^A/\varepsilon_f^B < 1$ , and the  $B_{2u}$  state becomes the ground state. The  $B_{2u}$  and  $B_{3u}$  splitting is much larger, around 30K, in agreement with [7]. We used  $\varepsilon_f^B = 110$  K,  $\varepsilon_f^A \approx 80$  K [7], and we use the same value for  $N_0$ .

*Anisotropy Switch at High T* – Due to the existence of two regimes for conductivity, hopping and Drude, a switch of anisotropies is expected to occur at high  $T$  [10]. For  $x = 0.02 - 0.04$ , we find  $\sigma_A > \sigma_B$  at very low  $T$ , since they all have a  $B_{2u}$  ground state, while  $\sigma_A < \sigma_B$  at high  $T$  [10], since  $\langle n_{2D}^A \rangle < \langle n_{2D}^B \rangle$ , see Fig. 3. For  $x = 0.01$ , which has a  $B_{3u}$  ground state, the same analysis apply.

However, since  $\langle n_{2D}^A \rangle$  is only slightly larger than  $\langle n_{2D}^B \rangle$ , we observe a smooth convergence of conductivities for  $120 < T < 250$  K, Fig. 3, and a regime with  $\sigma_A > \sigma_B$  would occur only at much higher  $T$  (not measured).

The values for  $n_{3D}^0 = n_{2D}^0/c_0$ ,  $m^* \approx 4m_e$ , and  $\varepsilon_f^{A,B}$ , are all consistent with Hall coefficient [22] and optical conductivity [7, 23].

*Conclusions* – In lightly doped  $\text{La}_{2-x}\text{Sr}_x\text{CuO}_4$ , correlations open a Mott gap in the spectrum, place the top of the valence band close to  $(\pm\pi/2, \pm\pi/2)$ , and stabilize a parity-odd ground state. Once the stage is set, the peculiar AC and DC responses can be promptly described using basic concepts from  $p$ -type semiconductor physics. In particular, all the novel anisotropies arise from the parity-odd, rotational-symmetry-broken deep and shallow acceptor levels, which are split by orthorhombicity.

*Acknowledgements* – M. B. S. N. acknowledges discussions with J. Falb, R. Gooding, A. Muramatsu, and O. Sushkov. Y. A. is supported by KAKENHI 19674002 and 20030004.

---

\* Electronic address: barbosa@itp3.uni-stuttgart.de

- [1] P. A. Lee, N. Nagaosa, and X.-G. Wen, *Rev. Mod. Phys.* **78**, 17 (2006).
- [2] J. Chang, *et al.*, arXiv:0805.0302 [cond-mat.supr-con].
- [3] N. Doiron-Leyraud, *et al.*, *Nature* **447**, 565 (2007).
- [4] C. Jaudet, *et al.*, *Phys. Rev. Lett.* **100**, 187005 (2008).
- [5] A. Comanac, *et al.*, *Nature Physics* **4**, 287-290 (2008).
- [6] A. Lavrov, *et al.*, *Phys. Rev. Lett.* **87**, 017007 (2001); A. Gozar, *et al.*, *Phys. Rev. Lett.* **93**, 027001 (2004); Yoichi Ando, *et al.*, *Phys. Rev. Lett.* **93**, 267001 (2004).
- [7] M. Dumm, *et al.*, *Phys. Rev. Lett.* **91**, 077004 (2003); W. J. Padilla, *et al.*, *Phys. Rev. B* **72**, 205101 (2005).
- [8] Yoichi Ando, *et al.*, *Phys. Rev. Lett.* **87**, 017001 (2001).
- [9] D. N. Basov, B. Dabrowski, and T. Timusk, *Phys. Rev. Lett.* **81**, 2132 (1998).
- [10] Yoichi Ando, *et al.*, *Phys. Rev. Lett.* **88**, 137005 (2002).
- [11] V. Kotov and O. P. Sushkov, *Phys. Rev. B* **72**, 184519 (2005).
- [12] B. I. Shklovskii and A. L. Efros, in *Electronic Properties of Doped Semiconductors*, Springer Verlag (1984).
- [13] K. M. Rabe and R. N. Bhatt, *J. Appl. Phys.* **69**, 4508 (1991).
- [14] R. J. Gooding, *Phys. Rev. Lett.* **66**, 2266 (1991).
- [15] Yan Chen, T. M. Rice, and F. C. Zhang, *Phys. Rev. Lett.* **97**, 237004 (2006).
- [16] W. Kohn and J. M. Luttinger, *Phys. Rev.* **98**, 915 (1955).
- [17] O. P. Sushkov, *et al.*, *Phys. Rev. B* **77**, 035124 (2008).
- [18] M. B. Silva Neto, *et al.*, in preparation.
- [19] A. Gozar, Seiki Komiya, Yoichi Ando, and G. Blumberg, in *Frontiers in Magnetic Materials*, ed. A. V. Narlikar, pp. 755-789, Springer-Verlag, 2005.
- [20] E. Lai and R. J. Gooding, *Phys. Rev. B* **57**, 1498 (1998).
- [21] V. Ambegaokar, B. I. Halperin, and J. S. Langer, *Phys. Rev. B* **4**, 2612 (1971).
- [22] Yoichi Ando, *et al.*, *Phys. Rev. Lett.* **92**, 197001 (2004).
- [23] W. J. Padilla, *et al.*, *Phys. Rev. B* **72**, 060511(R) (2005).